TiO_2 wheat-like arrays by anodizing a sputtered Ti membrane on FTO substrate and its application in dye-sensitized solar cells

CUIPING KANG*, BING DU, ZHIHUAI YANG
Nonlinear Research Institute, Baoji University of Arts and Sciences, Baoji 721016, China

TiO_2 wheat-like arrays were prepared by anodizing a sputtered Ti membrane. The current-time curves show the growing process of TiO_2 arrays, in which the controllable growth technique is studied for obtaining a satisfied product. Then TiO_2 wheat-like arrays were applied in dye-sensitized solar cells (DSSCs) and the photovoltaic performance of DSSC with different film thickness were investigated. The results show that the short-circuit current density (J_{sc}) and the total energy conversion efficiency (η) increase but the fill factor (FF) decrease as the increase of the film thickness, which could be attributed to the increase of the specific surface areas and the increase of electron losses by the increase of film thickness, respectively.

(Received July 4, 2014; accepted September 29, 2016)

Keywords: TiO_2 wheat-like arrays, Sputtered, Anodization, Dye-sensitized solar cells

1. Introduction

Dye-sensitized solar cells (DSSCs) have attracted great interest in academic research and industrial applications due to their higher efficiency, potentially lower cost, and improved environmental friendliness compared to traditional silicon solar cells [1-3]. As one of the most important part of DSSC, photoanode has been investigated with greatest enthusiasm in recent years [4-6]. Absorbing dyes as much as possible and direct electron transport capability are needed for an optimized photoanode [7-9]. One dimensional nano-structure such as nanotube has been studied for improving electron transport capability [10-12]. However, one-dimensional structural result to a remarkable decrease of absorbed dye, which is adverse for DSSC efficiency [12-14]. Photoanode with the combining advantages are needed for high-efficiency DSSC at present [15-17].

In our work, TiO_2 wheat-like arrays, which can be considered as a quasi one-dimensional structure, were prepared by potentiostatic anodization and applied in dye-sensitized solar cells. The quasi one-dimensional structure possesses a larger specific area and direct electron transport route, which is optimized structure for high-efficiency DSSC. The controllable growth rules were studied for a longer length and the thickness dependent DSSC were discussed for a higher efficiency.

2. Experimental

The Ti membrane were obtained by sputtering Ti onto a cleaned fluorine-doped tin oxide transparent conducting (FTO) glass by DC magnetron sputtering with a high purity titanium target. The sputtering power was set as 40 W and the time was set as 0.5 h, 1h, 1.5h, 2 h to obtain Ti membrane with different thickness.

Then the sputtered Ti membrane was accepted to a two-electrode electrochemical system for potentiostatic anodization. Ti membrane was act as photoanode and a metallic Ti sheet was used as photocathode. They were dipped into electrolyte of a stirred 0.3 wt% NH_4F contained ethylene glycol solution. Anodization was performed at 50V under stirring with the environmental temperature of 0°C. As strictly monitoring process parameters to a same condition for all film with different thickness, we obtained TiO_2 wheat-like arrays without exception. Then the annealed samples in 450 °C were applied in DSSCs for photovoltaic performance test.

The morphology of the samples was investigated by field-emission scanning electron microscopy (FESEM) (Hitachi, S-4800). The thickness of the samples was measured by a step profiler. Raman scattering spectra were measured on a Jobin-Yvon LabRam HR800 spectrometer (with a 532 nm of yttrium aluminum garnet (YAG) laser as the exciting light source). Photocurrent–voltage characteristics of the cells were measured under an illumination of AM 1.5 (1 Sun, 100mW/cm^2) using a solar light simulator.

3. Results and discussion

3.1. Morphological and structural characterization of TiO_2 wheat-like film

Fig. 1 is the schematic diagram of the growth of TiO_2 wheat-like arrays. Fig. 1a shows the morphology of Ti membrane before anodization as magnifying presentation of Fig.3A in photograph. The growth of TiO_2 wheat-like arrays is just like the growth of nanotube, whose direction is vertical to the substrate. The onset of anodization, a thin layer of oxide forms on the titanium membrane surface and then some tiny pits originate in the surface growing into inner (Fig.1b). The tiny pits decrease the thickness of the membrane which result to a enhanced electric field intensity in such pits and thus result to a further pore growth. As the growth go on, a stem-like structure (as is showed in Fig. 1c) forms. Meanwhile, the inhomogeneity of Ti membrane also results to a lateral development of nano stem-like structure to form a wheat-like structure (as shown in Fig. 1d). However, the horizontal field intensity is weaker than the field intensity vertical to substrate, so the lateral growth is weaker than the vertical growth, especially in stem bottom.

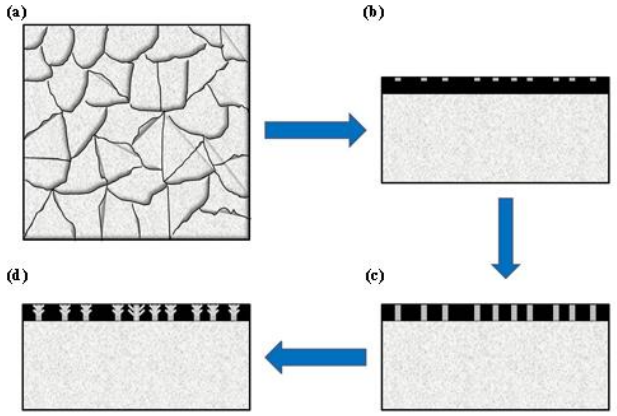

Fig. 1. Schematic diagram of the growth of TiO_2 wheat-like arrays: (a) original Ti membrane; (b) small pinks in Ti membrane; (c) the stem-like structure; (d) the wheat-like structure

Fig. 2 shows the morphologies of TiO_2 wheat-like arrays. Fig. 2a and Fig. 2c show the lateral images of TiO_2 wheat-like arrays. The structures are vertical to the substrate with a wheat-like structure: The top layer shows a densely one-diameter liner structure and the bottom layer shows a rough stem-like structure. Fig. 2b shows top-surface view of TiO_2 wheat-like structure. It displays much interspace between the stems. Fig. 2d shows a small segment from the membrane. It shows a densely arrays and much large pore space between them.

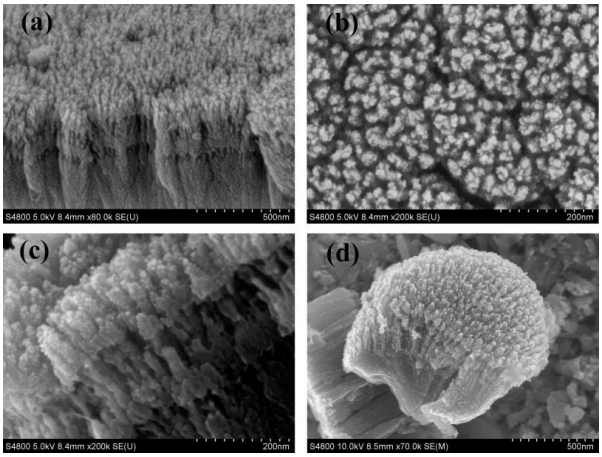

Fig. 2. SEM images of TiO_2 wheat-like arrays by anodization: (a), (c) cross-section, (b) top surface, (d) a slice section

Fig. 3 shows the photograph comparison of Ti membrane before anodization and the TiO_2 wheat-like arrays after anodization. We can see from the graph that the Ti membrane before anodization is black and opaque. On the contrary, the TiO_2-arrays membrane after anodization is transparent with a light color. It indicates the difference between the Ti structure and TiO_2 structure.

Fig. 3. Photographs of the samples before and after anodization: (A) Ti membrane before anodization; (B) TiO_2 wheat-like arrays after anodization

Fig. 4 shows the Raman scattering spectrum of TiO_2 wheat-like arrays after annealing at 450 °C. It can be observed that there are five Raman peaks in 144 cm^{-1}, 196 cm^{-1}, 396 cm^{-1}, 515 cm^{-1}, 640 cm^{-1}, which should be assigned to the E_g, E_g, B_{1g}, $A_{1g}+B_{1g}$ and E_g mode, respectively [16,17]. It indicated that the annealed samples reveal the only anatase phase. The unannealed samples show amorphous state.

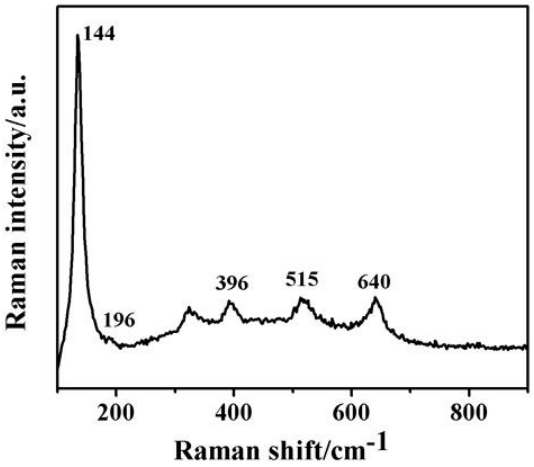

Fig. 4. Raman scattering spectrum of TiO_2 wheat-like arrays after annealing at 450°C for 3h in air

3.2. The growth rule and controllable growth technique of TiO_2 wheat-like arrays

In the anodization process of TiO_2 forming, the current-time curves (I-t curves) were recorded as Fig. 5. It can be divided into five sections generally. Section a displays the formation of barrier layer. In this section, the current decreased immensely with increase of the barrier layer, which will hinder the growth of TiO_2 arrays. Section b is a etching process of barrier layer. Many tiny pits form in this section. The pits decrease the thickness of barrier layer and thus lead to a rise to current, which indicates a rising growth with TiO_2 wheat-like arrays. Section c is another growth stage of TiO_2 wheat-like arrays. In this stage, the growth is going on but the barrier layer is thicker result to a decreasing growth speed of TiO_2 wheat-like array that lead to a drop to current again. Section d is a stable growth stage. The barrier reaches the largest thickness in this stage, so the current would not change again. Section e is the stage of TiO_2 arrays dissolve, which obviously increase the current due to the decreasing of thickness of barrier.

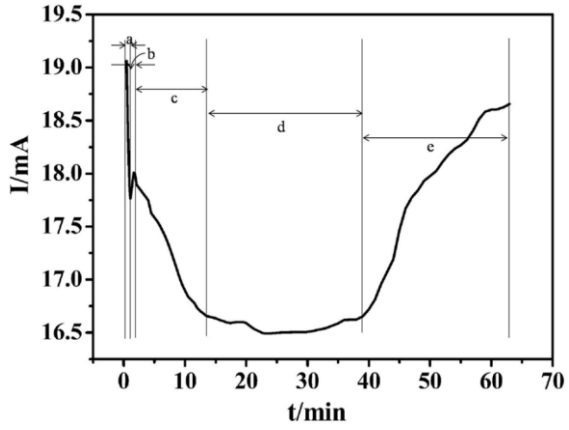

Fig. 5. Current-time curve of TiO_2 wheat-like arrays in anodization process

From Fig. 5, we could obtain much useful information for the growth of TiO_2 wheat-like arrays from I-t curves such as identify the growth stage or obtain the largest thickness etc. Accordingly, we could control the growth process for the most optimized structure and a longer length according to I-t curves. In our experiment, based on the characteristics of the growth process of membrane, we got the largest thickness film in anodization process by controlling the growth process to process d.

3.3. The photovoltaic performance of TiO_2 wheat-like arrays based DSSCs

The photovoltaic-characteristics depending on the membrane thickness are displayed in Fig. 6. As the film thickness increases, the short-circuit photocurrent density (J_{sc}) increases as well (Fig. 6a). However, the open-circuit voltage (V_{oc}) shows a decline trend in general (Fig. 6b) and the fill factor (FF) decreases in invariably trend (Fig. 6c). The variation of J_{sc}, V_{oc} and FF embodies the variation trend of the total energy conversion efficiency (η). The obvious increasing trend of J_{sc} results to an obvious increase trend of the total energy conversion efficiency (η). (Fig. 6d)

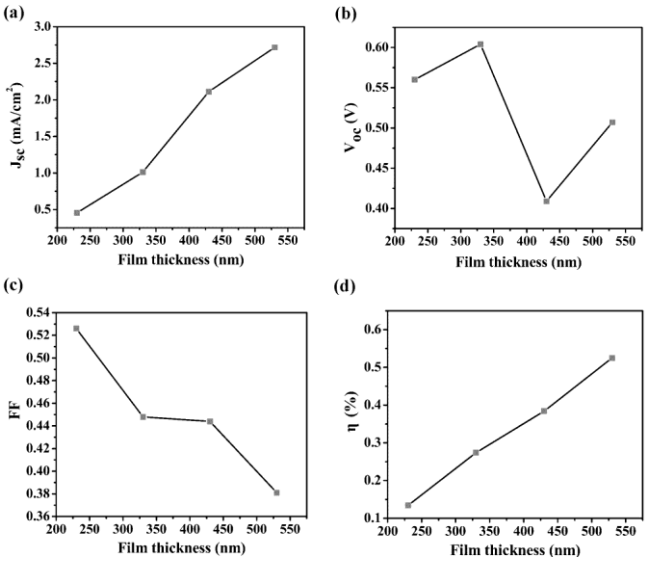

Fig. 6. Film thickness dependent photovoltaic characteristics relationships: J_{sc} (a), V_{oc} (b), FF (c) and conversion efficiency (η) (d)

The photocurrent density-photovoltage characteristic curves (*J–V* curves) of DSSCs based on annealed TiO_2 film with different thickness are displayed in Fig. 7. From the J-V curves, we can get the largest efficiency of 0.525% by the thickest film of 530 nm. The efficiency decreases extremely when film thickness decrease.

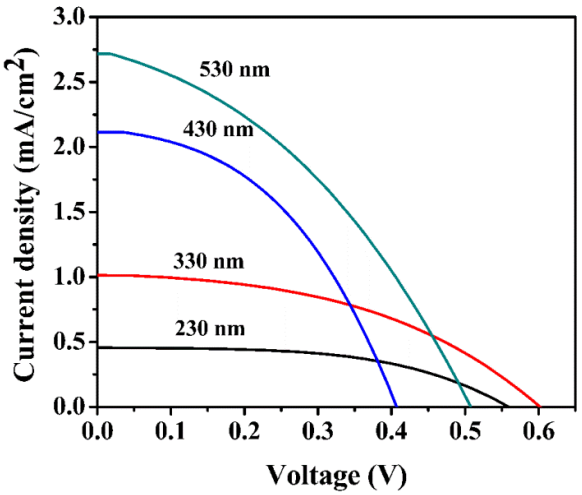

Fig. 7. J–V curves of DSSCs based on annealed TiO_2 film with different thickness

In our experiment, the film thickness is at a region of 230 nm to 530 nm, which are much thinner for a high-efficiency DSSC. The variation of the film thickness reflects variation of the specific surface areas and larger thickness corresponds to larger specific surface areas. Accordingly, a larger film thickness may bring in improved total energy conversion efficiency. However, the film quality become worser when the film thickness increase, which leads to more flaws and thus to more leakage current. These factors increase charge transport loss and dark current, and thus decrease FF obviously. Therefore, increasing the film thickness to a larger J_{sc} and controlling film quality for a larger FF are the two keys for higher DSSC efficiency.

4. Conclusion

In summary, we have successfully prepared the TiO_2 wheat-like arrays by anodizing a sputtered Ti membrane and applied it in dye-sensitized solar cells. The current-time curve (I-t curves) indicates the controllable growth process of TiO_2 arrays. The photovoltaic characterization of TiO_2 arrays based DSSC shows an improved DSSC efficiency with the increase of film thickness, which can be attributed to the sharply increase of short-circuit current. However, the decrease of fill factor (FF) decreases total efficiency to some extent. Accordingly, further increase the film thickness and control film quality can increase DSSC efficiency immensely.

Acknowledgements

This work is supported by Scientific research plan projects of Education Department of Shaanxi province of China (Grant No. 12JK0983), Natural Science Basic Research plan in Shaanxi Province of China (Grant No. 2012JQ1011) and Key projects of Baoji university of arts and sciences (Grant No. ZK12047).

References

[1] B. O'Regan, M. Grätzel, Nature **353**, 737 (1991).
[2] M.Grätzel, J. Photochem. Photobiol. C **4**, 145 (2003).
[3] M. Grätzel, J. Photochem. Photobiol. A **164**, 3 (2004).
[4] C. Y. Jiang, X. W. Sun, G. Q. Lo, D. L. Kwong, Appl. Phys. Lett. **90**, 263501 (2007).
[5] R. H. Tao, J. M. Wu, H. X. Xue, X. M. Song, X. Pan, X. Q. Fang, X. D. Fang, S. Y. Dai, J. Power Sources **195**, 2989 (2010).
[6] T. W. Hamann, A. B. F. Martinson, J. W. Elam, M. J. Pellin, J. T. Hupp, J. Phys. Chem. C **112**, 10303 (2008).
[7] D. J. Yang, H. Park, S. J. Cho, H. G. Kim, W. Y. Choi, J. Phys. Chem. Solids **69**, 1272 (2008).
[8] K. Zhu, N. Kopidakis, N. R. Neale, J. Lagemaat, A. J. Frank, J. Phys. Chem. B **110**, 25174 (2006).
[9] K. Zhu, N. R. Neale, A. Miedaner, A. J. Frank, Nano Lett. **7**, 69 (2007).
[10] J. J. Wu, G. R. Chen, H. H. Yang, C. H. Ku, J. Y. Lai, Appl. Phys. Lett. **90**, 213109 (2007).
[11] H. Wang, C. T. Yip, K. Y. Cheung, A. B. Djurišić, M. H. Xie, Appl. Phys. Lett. **89**, 023508 (2006).
[12] A. B. F. Martinson, J. W. Elam, J. T. Hupp, M. J. Pellin, Nano Lett. **7**, 2183 (2007).
[13] Y. Gao, M. Nagai, T. C. Chang, J. J. Shyue, Cryst. Growth Des. **7**, 2467 (2007).
[14] H. M. Cheng, W. H. Chiu, C. H. Lee, S. Y. Tsai, W. F. Hsieh, J. Phys. Chem. C **112**, 16359 (2008).
[15] C. H. Ku, J. J. Wu, Appl. Phys. Lett. **91**, 093117 (2007).
[16] D. A. Wang, B. Yu, F. Zhou, C. W. Wang, W. M. Liu, Mater. Chem. Phys. **113**, 602 (2009).
[17] K. M. Lee, V. Suryanarayanan, J. H. Huang, K. R. J. Thomas, J. T. Lin, K. C. Ho, Electrochim. Acta **54**, 4123 (2009).

*Corresponding author: kangcp06@126.com